Geomorphology 471 (2025) 109576

Contents lists available at ScienceDirect

Geomorphology

journal homepage: www.journals.elsevier.com/geomorphology

Gypsum cave notches and their palaeoenvironmental significance: A combined morphometric study using terrestrial laser scanning, traditional cave mapping, and geomorphological observations

Jorge Sevil-Aguareles [a,*], Luca Pisani [b], Veronica Chiarini [c], Tommaso Santagata [d], Jo De Waele [e]

[a] Departamento de Ciencias de la Tierra, Universidad de Zaragoza, C/. Pedro Cerbuna 12, 50009 Zaragoza, Spain
[b] Centro di Documentazione Speleologica "F. Anelli", Società Speleologica Italiana, Via Zamboni 67, 40126, Bologna, Italy
[c] Department of Geosciences, University of Padua, Via G. Gradenigo 6, 35131 Padova, Italy
[d] VIGEA - Virtual Geographic Agency, 42123 Reggio Emilia, Italy
[e] Bologna University, Department of Biological, Geological and Environmental Sciences (BIGEA), Via Zamboni 67, 40126 Bologna, Italy

ARTICLE INFO

Keywords:
Karst
Evaporite
Dissolution
Geomorphology
Paleohydrology

ABSTRACT

Terrestrial laser scanning has shown to be a very powerful method for the study and monitoring of caves. The high density of acquired points allows geostatistical methods to be used in the elaboration of large datasets on different depositional and erosional morphologies on cave walls, roof and floor. Here we describe a multidisciplinary morphometric study on cave wall morphologies and sediments in a multi-level gypsum cave system in the northern Apennines (Italy) with the objective of finding the direction of water flow that created these passages over hundred thousand years ago. The analysis of the traditional cave map (in long profile) suggests an overall, albeit very low, north-west inclination of the cave passages. However, other definitive indicators of flow direction, such as scallops, are absent which restricts the verification of this interpretation. The laser scanner-derived 3D point clouds of the cave wall notches of the main level have been analysed using different methods to verify the paleocurrent direction. However, statistical analyses of the point cloud data have yielded inconclusive results, even if most flow-related morphologies appear to be gently sloping towards north-west, where the present main cave entrance is found. Imbrication of fluvial sediments prevalently indicates the same direction. While no single method provided conclusive results on its own, the collective evidence strongly suggests an ESE to WNW paleocurrent flow, confirming the ancient resurgence nature of the cave gallery.

1. Introduction

Karst areas are generally characterised by a strong interconnection between hydrology and geomorphology, with an underground drainage strongly affected by the surface morphology and vice versa (Ford and Williams, 2007; De Waele and Gutiérrez, 2022). This is particularly true for epigenic carbonate karst, in which the dissolving power of the fluids mainly derives from surface CO_2, and meteoric waters enter the soluble formation from above, dissolving the rocks and creating an aquifer with a double, or even triple, porosity (White, 2002).

Epigenic gypsum karsts are somewhat different from those developed in carbonates: evaporites (i.e., gypsum rocks) have very low porosity (Klimchouk, 1996), they are characterised by more widely spaced fractures (Pisani et al., 2019), and they dissolve readily in water independently of CO_2. This produces aquifers with a different behaviour with respect to carbonate karst (Vigna et al., 2017), and cave systems with rather similar morphologies, but with some distinctive shapes and differences (e.g., Urban et al., 2009; Calaforra and Gázquez, 2017). The faster dissolution of gypsum with respect to carbonates gives epigenic gypsum caves a unique evolution, which, coupled with the stratigraphic and structural settings, creates characteristic networks of passages. Landscape evolution in gypsum areas in temperate climate zones can be extremely rapid, allowing to infer environmental changes over short periods of time, such as a few thousand years (Columbu et al., 2017). In carbonate karst, on the contrary, caves need longer times to form and adjust to changing base levels, allowing landscape reconstructions only over longer time scales in the order of 10^5–10^6 years (Rixhon, 2023).

It is worth emphasising that cave evolution in gypsum areas in

* Corresponding author.
E-mail addresses: jorgesevil@unizar.es, jorge.sevil.aguareles@gmail.com (J. Sevil-Aguareles), lucapiso94@gmail.com (L. Pisani), veronica.chiarini3@gmail.com (V. Chiarini), tommaso@vigea.it (T. Santagata), jo.dewaele@unibo.it (J. De Waele).

https://doi.org/10.1016/j.geomorph.2024.109576
Received 14 October 2024; Received in revised form 11 December 2024; Accepted 11 December 2024
Available online 12 December 2024

temperate climate is rapid, especially shortly after colder periods, when rainfall increases and more sediment is moved into the karst due to the still scarce vegetation cover (Columbu et al., 2015). This sediment transport increases the (physical) erosional power of the entering waters, enlarging cave conduits also via mechanical erosion. These periods of sediment entrainment into the caves also causes increased alluviation in the conduits and the related antigravitative (upward and sideward) enlargement of the active passages (Pasini, 2009; Farrant and Smart, 2011). Warmer climate, on the contrary, increases CO_2 concentrations in the soils leading to calcite speleothem precipitation in previously carved gypsum voids (Columbu et al., 2015). Contrarily, caves form more easily during warmer periods in limestone areas, because of the increased CO_2 contents in the soils and higher precipitation, increasing the solubility of carbonate minerals (Harmand et al., 2017). In rather rapidly uplifting areas, the interplay between tectonics and changing climate gives rise to multi-level karst systems, with underground river passages rapidly adjusting to changes in base-levels, in limestone karst areas (Calvet et al., 2015), but especially in gypsum caves (Columbu et al., 2015, 2017; Pisani et al., 2019).

Mature underground streams in caves, especially in areas where recharge is continuous and rather uniform (with poor seasonal contrasts in hydrological regime), close to their terminal parts (towards the spring), are often characterised by very low gradients, as low as <0.1 %, with passage floors very close to the horizontal (Audra and Palmer, 2015). Sometimes outlets can be accessible, allowing speleologists to enter the resurgences and follow the rivers upstream over variable distances. Ancient resurgences, no longer active, can be found hanging high on cliffs or valley slopes, and these dry passages are what is left of the underground karst network after a base level lowering occurred. These old outflows and cave levels can host sediments which allow to date the speleogenetic phases (although sediments and speleothems only give indications of a minimal age of the conduits they occupy), and the connected landscape evolution (Haüselmann et al., 2007; De Waele et al., 2012).

Recognising the ancient function of a fossil cave passage (spring or sink) relies on the general altitudinal profile of the cave passage (rising or descending), the identification of original flow marks on the walls, floor and ceiling (i.e., scallops), or the sedimentological markers of flow directions (i.e., direction of the imbrication of fluvial clasts). These flow direction markers can be missing completely (eroded by later processes or erased by condensation-corrosion phenomena, e.g. Cailhol et al. (2019) and Columbu et al. (2021)), or can be hidden from view (covered with more recent sediments or speleothems). In such cases the general inclination of the passages can indicate the direction of flow, especially if they extend over considerable distances. Classical cave survey methods are typically sufficient to resolve the spring/sink enigma in most cases.

In this paper we report a case study of a relict gypsum cave passage opening around 83 m above the regional base level. This passage develops in an eastward direction for over 300 m with dimensions of 0.5–5 m width and 2–15 m height, continuing with a narrow passage <0.5 m high. Based on cave surveys, its longitudinal profile, which is disturbed by rockfalls, sediments, and displacements, does not allow to identify its descending or ascending nature. Besides, scallops are missing (due to the macrocrystalline nature of the gypsum rock), and clearly imbricated cave sediments do not give an unequivocal answer regarding the flow direction. Although in previous studies it has always been considered a resurgence due to its geological setting (Columbu et al., 2015), some observations and local measurements carried out by cave explorers rose the hypothesis of the presence of an opposite gradient, which might have pointed to the cave as a sink and not a resurgence. In this regard, our main objective was to explore the potential of terrestrial laser scanner (TLS) surveys in (1) quantifying, with geostatistical methods, the overall morphometry of wall notches and antigravitative ceiling channels as indicators of ancient water flow direction, and (2) overcoming the limitations associated with conventional topographic cave surveying. In this karst area, laser scanning has already allowed to study an archaeological cave used for the extraction of "*lapis specularis*" during roman age, a sort of gypsum glass (Santagata et al., 2015), the speleogenetic evolution of a gypsum cave (Ca' Castellina Cave, De Waele et al., 2018) and of a roman gypsum quarry in the Monte Mauro area (Fabbri et al., 2021).

2. Study area

2.1. Gypsum karst of Romagna

Evaporite karst areas in Emilia-Romagna mainly outcrop on the northern edge of the Apennines (Messinian gypsum) and along the Upper Secchia Valley (Triassic gypsum). The largest of these areas occur south of the city of Bologna (the *Gessi Bolognesi e Calanchi dell'Abbadessa* Regional Park), and south-west of the cities of Imola and Faenza, ca. 50 km south-east of Bologna (the *Vena del Gesso Romagnola* Regional Park).

This region represents the most studied evaporite karst area in the world and has been the focus of scientific research since the late 16th century. Thanks to its unique geological and naturalistic features and its scientific importance it has been declared a UNESCO world heritage site in 2023 under the name "Evaporitic Karst and Caves of Northern Apennines" (EKCNA) (https://whc.unesco.org/en/list/1692). EKCNA has become the only Italian site with a strong karst and speleological imprint to be included in the UNESCO list, and the first karst site in evaporites (gypsum) in the world.

The *Vena del Gesso Romagnola* is an important outcrop of Messinian gypsum developing for about 25 km along a W/NW-E/SE direction. In this area there are approximately 300 registered caves, for a total of 48 km of development. This geological formation is made of 16 gypsum beds separated by clayey interlayers and deposited during the Messinian salinity crisis (Lugli et al., 2008).

Our study site, the Re Tiberio Cave system, is situated in the central portion of the *Vena del Gesso Romagnola* Regional Park, close to the village of Borgo Rivola. In this area the original sedimentary sequence is strongly fractured and has undergone stacking as a consequence of ancient submarine landslides (Roveri et al., 2003), reaching a thickness up to 350 m and rising high above the local base level, which is represented by the Senio Stream. The latter cuts the gypsum outcrop perpendicularly along a N/NE-S/SW direction (Fig. 1).

2.2. The Re Tiberio Cave system

The Re Tiberio Cave system develops within the Monte Tondo area (Borgo Rivola, province of Ravenna) for over 7 km and can be defined a multi-level system, organised into 5 main sub-horizontal levels and 7 further potential ones of minor development (Columbu et al., 2015; Chiarini et al., 2022, 2024) (Fig. 1). This is the best developed epigenic karst system in the entire area of the *Vena del Gesso Romagnola* Regional Park. The main cave level, which opens at 180 m a.s.l., 83 m above the Senio Stream thalweg, has been equipped for tourist visits in its first 80 m. This initial part of the cave is of archaeological and historical interest (Sanna et al., 2023) and was scanned with a laser scanner already over 10 years ago (Canevese et al., 2013).

The local geological and geomorphological setting, characterised by an over 350 m thick evaporite sequence cut by a stream, constitutes an ideal condition for the preservation of the relationship between cave and surface landscape evolution. The studies carried out previously, based on the U/Th dating of calcite speleothems and on the comparison of the sub-horizontal levels of the caves and the river terraces of the Senio Stream, have highlighted the close link between the climatic conditions triggering the valley incision and aggradation in this uplifting area, and the evolution of the karst system (Columbu et al., 2015). The formation of karst conduits has been related to late Quaternary climatic oscillations on a millennial scale, establishing an evolutionary model that explains the formation of conduits with sub-horizontal development

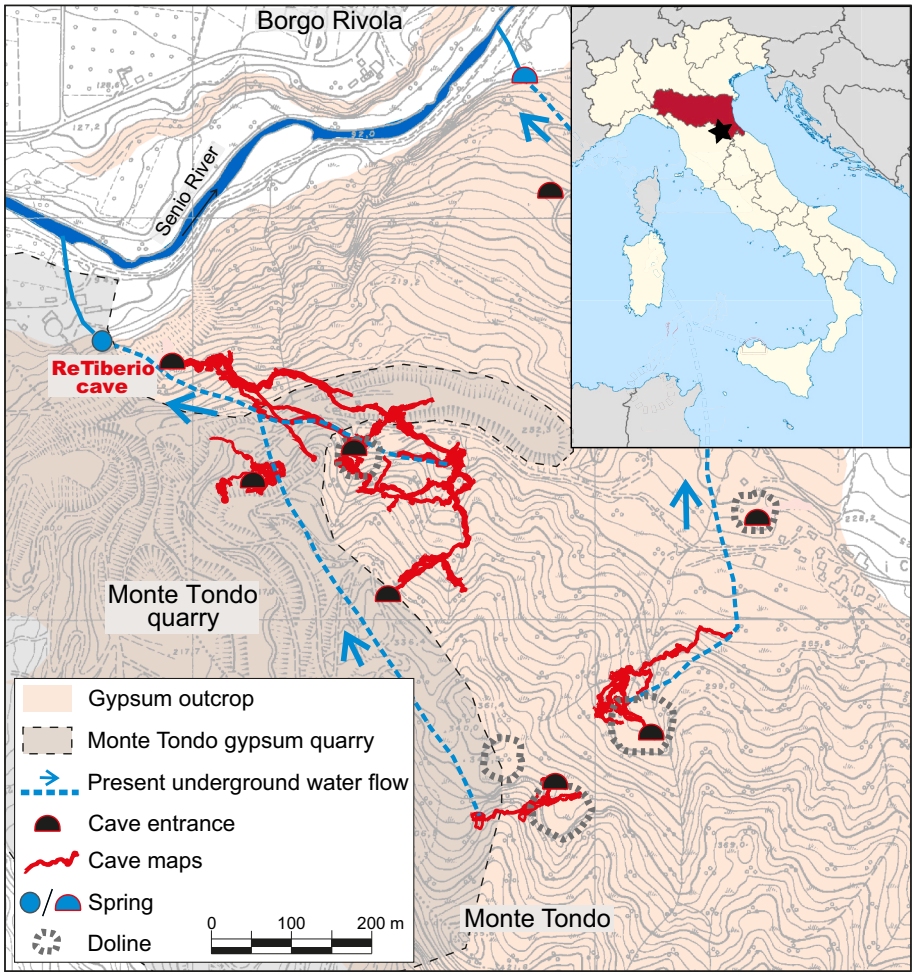

Fig. 1. Location of the Re Tiberio and neighbouring caves in the Monte Tondo karst area. Cave maps are shown in red, whereas blue arrows indicate present underground water flow. Note the cave is cut, in some of its parts, by the Monte Tondo gypsum quarry, in grey. The salmon area indicates the gypsum outcrop.

during periods characterised by a relatively cold climate, while in the warmer climate phases there is a slowdown of speleogenetic processes and a widespread growth of carbonate speleothems (Columbu et al., 2015, 2017). Based on the U/Th dating of speleothems, which give the minimum age of the cave level in which they formed, and a comparison with the record of fluvial terraces in the nearby valleys, this multilevel system formed during the last 300 ka (Chiarini et al., 2024).

All the previous studies have taken for granted that the natural entrance of the Re Tiberio Cave main gallery functioned as a spring during its formation. This agrees with the overall low gradient of the passage, which fits well with a final tract of an active cave branch close to its outlet. However, no other clear and evident univocal signs of flow direction, such as scallops or unidirectional imbricated river sediments, can be used to confirm this interpretation.

3. Methods

3.1. Cave survey and geomorphological observations

Although the focus of this work was to identify the direction of the stream which formed the main Re Tiberio Cave level, initial observations were made on the entire karst system to help the understanding of its evolution. A first step was the analysis of the topographic cave survey obtained between 1994 and 2003 with traditional techniques using combined clinometer-compass (Suunto) and 20-m measuring tape. The main levels of the cave were resurveyed during the past 6 years using the modern Disto-X laser range finder (Heeb, 2014), adjusting the new traverse line and thus improving the overall accuracy of the earlier survey. The cave survey is available online in the regional cadastre of natural cavities of Emilia-Romagna (https://geo.regione.emilia-romagna.it/schede/speleo/index.jsp?id=42100). The cave map was drawn analogically, then reproduced digitally using the 'resurvey' tool of the *cSurvey* software (Pisani and Lucci, 2022). The digitalised and georeferenced survey was used to extract the X, Y (coordinates) and Z (altitude) data of the most represented and continuous sub-horizontal galleries. Five main cave levels (corresponding to those in Columbu et al., 2015) were extracted. The data have been analysed using Excel software to calculate an average topographic gradient through the realisation of diagrams plotting the cumulative linear distance from the origin of each survey station vs. its altitude. For each cave level we calculated a linear trendline, where the angular coefficient represents an approximation of the topographic gradient.

Further analyses were carried out by direct geomorphological observations in the cave. Notches, flat ceilings, sediments, ceiling pendants and other relevant geomorphological and depositional elements were mapped. In this paper, we use the term notch to refer to vadose and antigravitative wall notches, also known as solution ramps. These morphologies are sub-horizontal recesses in the cave walls with a general slope having the same dip and dip direction of the cave stream that generated them (De Waele and Gutiérrez, 2022). Considering the limits of the method, which does not allow for a precise mapping and identification of very low gradients using analogical instruments in caves, further investigations were planned to extract detailed morphometric data. Fluvial deposits were also mapped and, when present, imbrication

was observed and its direction measured. This allowed to verify the flow direction of the water that deposited these sediments.

3.2. Laser scan acquisition

Laser scanner acquisition was carried out only in the main Re Tiberio Cave level using three different laser scanners. The area near the cave entrance and the initial tourist section were scanned using a Leica P40 Scan Station (9 scan stations) (Fig. 2A) and a Leica BLK360 laser scanner (80 scan stations) (Fig. 2B).

Leica P40 ScanStation is a terrestrial laser scanner equipped with an internal camera able to produce HDR 360° panoramic images used to colour the point clouds. This instrument can measure at distance of >250 m in very high resolution (<3 mm at 10 m distance) and short time

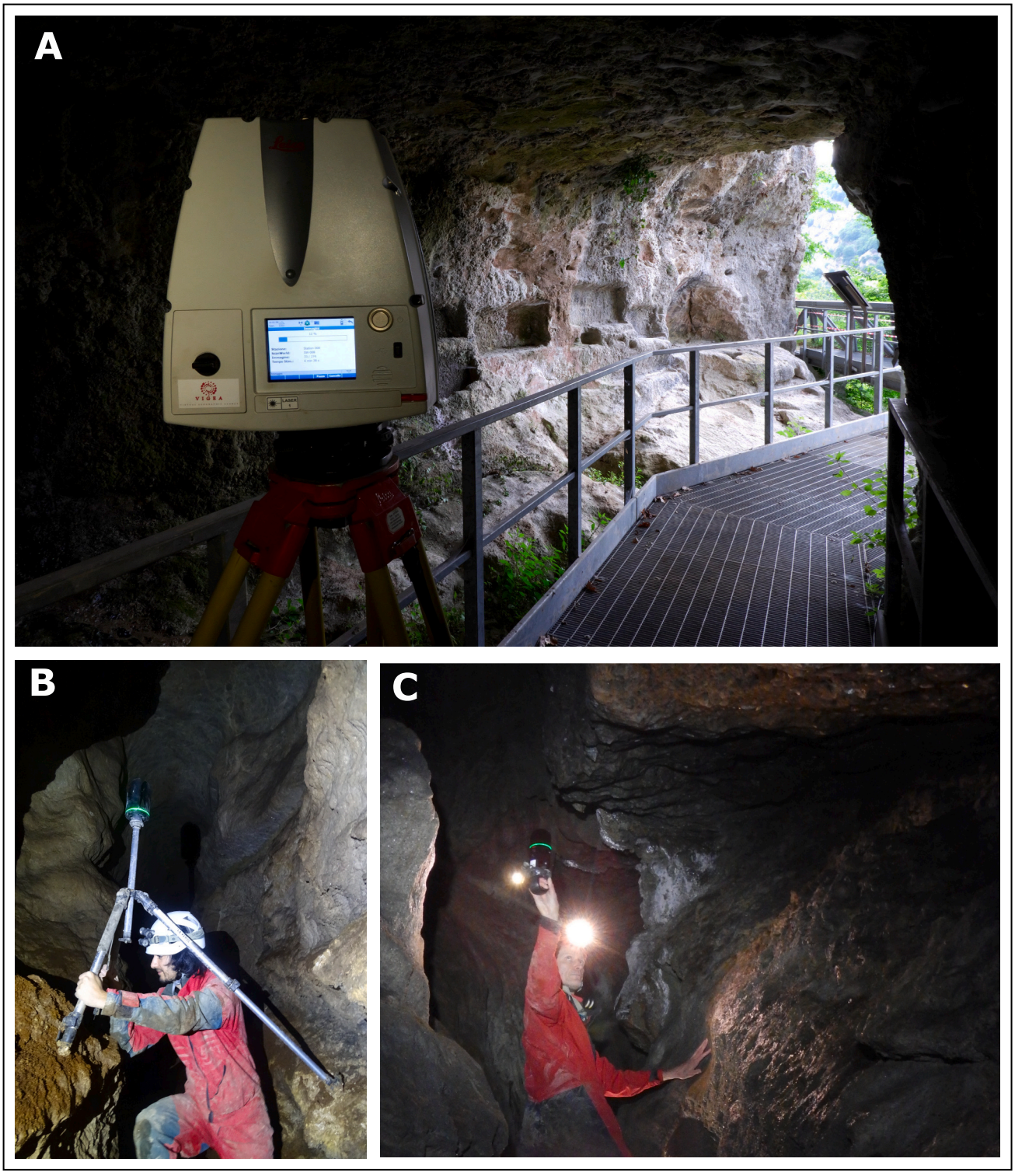

Fig. 2. The laser scanners used to map the Re Tiberio Cave: A. The Leica ScanStation P50 in the entrance area (Photo Tommaso Santagata); B. The Leica BLK360, placed on its tripod over a narrow and deep canyon (Photo Jo De Waele); C. The BLK2GO held in hand during the scanning of a narrow canyon-like passage (Photo Jorge Sevil-Aguareles).

(Santagata et al., 2022a). Considering the large size and weight of this laser scanner (about 20 kg including instrument and tripod) it was not possible to proceed in the lowest and most tortuous areas of the cave. For these reasons the BLK360 was used as a support in the most inaccessible areas whereas the Leica P40 scan station was used to 3D scan the largest areas.

Unlike most laser scanners, the Leica BLK360 has extremely small dimensions (height about 26 cm, width 11 cm and weight <1.5 kg) and is equipped with internal cameras for the acquisition of 360° panoramic and 180° thermal photographs. This instrument scans up to a distance of about 60 m in a period of time ranging from 3 to 7 min depending on the settings of the scanner and the internal cameras, with which it is possible to create panoramic photographs also in HDR. The possibility of using this instrument in caves makes data acquisition operations extremely easier and faster (Santagata et al., 2022b).

The sections of the small tunnels with complicated passages due to the presence of boulders and reduced widths were scanned using the BLK2GO hand-held laser scanner (Fig. 2C). Unlike TLS, hand-held scanners are instruments that allow to provide 3D point clouds of the environment while walking through it. In small caves, this kind of technology can be used for the almost total acquisition of the environment thanks to the possibility of moving much more comfortably and in extremely faster times, even if the data resolution is much less defined compared to tripod-based TLS instruments.

Integrated with an Inertial Measurement Unit (IMU) and three cameras to obtain coloured point clouds, the BLK2GO allows to 3D map and acquire RGB data information at the same time simply by walking in the areas to be detected. The GrandSLAM (Simultaneous Localization And Mapping) technology integrated in the BLK2GO combines LiDAR SLAM, Visual SLAM and the IMU to achieve the mapping performance acquiring 420.000 points per second. Through the LIDAR SLAM, the BLK2GO identifies different surfaces with unique geometry in the LIDAR data that are used to analyse and calculate its 3D position during its use. As in all tools that use IMU and SLAM algorithms, the trajectory is calculated in order to build its surrounding map and localise the instrument location on the map at the same time. Moreover, through the Visual SLAM system, the three panoramic cameras identify similarities between consecutive images (common features) to calculate the movement of the scanner.

Paired with a tablet or a phone and through a dedicated application, the data acquired can be viewed as a preview of the results in real time. The BLK2GO application also allows to control the instrument and check the battery status. Photographs can be geo-tagged during scanning and later be viewed in the exported point clouds. The BLK2GO data can be exported in high or low resolution with the advantage of immediately obtaining a clean point cloud and without the classic sketches that are usually produced by mobile scanners equipped with SLAM systems.

Four walks of about 6–10 min were necessary to 3D scan the passages and an overlap area of about 100 m to connect the scans of the BLK2GO with those realised with TLS. Once acquired, the data obtained by the BLK2GO were transferred using a wi-fi connection and processed with Leica Cyclone software, the same used to process the TLS data. As well as importing data, Cyclone software allowed to align and process the point clouds obtaining maps and cross-sections or other operations as the realisation of TIN (Triangulated Irregular Network) meshes and contour lines. After the processing phases, data were exported in .LAS file format to be viewed and analysed with other software packages.

3.3. Point cloud analyses

From the point cloud dataset obtained through the laser scanner survey, a compound 3D model was generated using CloudCompare (CloudCompare 2.13, 2024) merging the registered point clouds captured along the scanned passage (Fig. 3A-C). The final 3D model was subsampled to a spatial resolution of 10 mm to reduce processing time and was georeferenced using the pre-existent speleological topographic survey.

Following point cloud registration and georeferencing, the next step was to manually identify and isolate the existing notches in the cave walls and ceiling. For the analysis of the notches and the antigravitative ceiling channels, we divided the 3D point cloud into nine sectors, named S1.1–3, S2.1–3, S3.1–3, containing segments of the passage of similar orientation. To facilitate their identification, we applied the CloudCompare ShadeVis and the Eye-Dome Lighting (EDL) tools. The first,

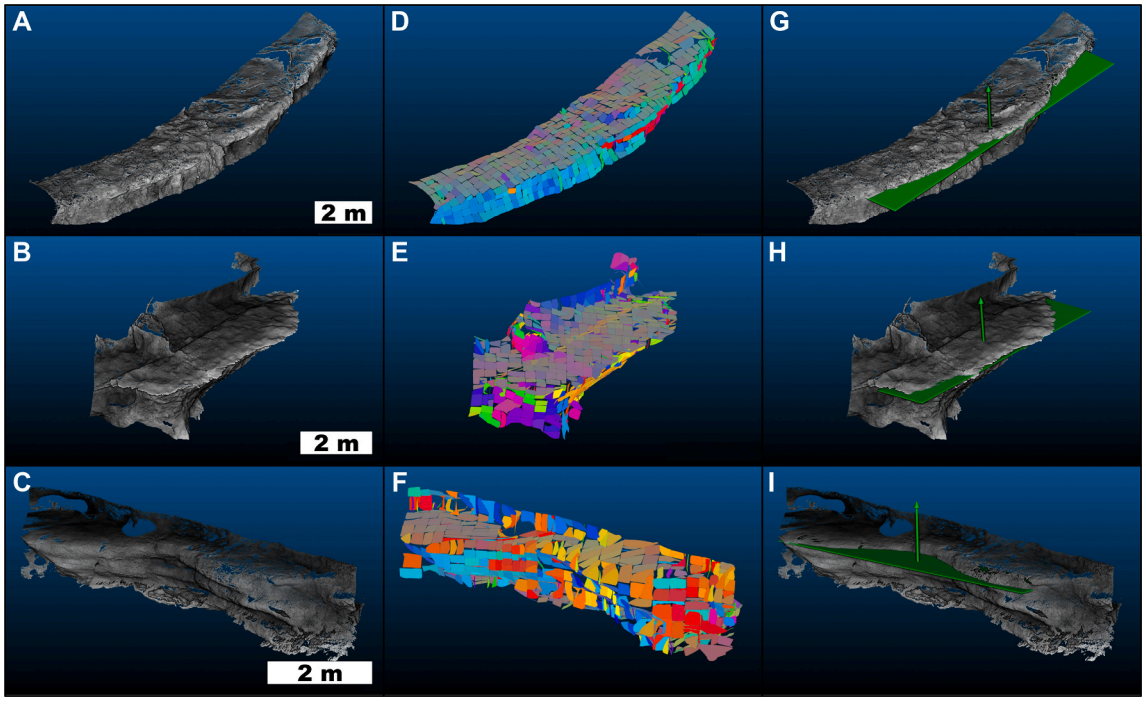

Fig. 3. Example of three different notches identified in the 3D point cloud (in greyscale; A, B, and C), together with their respective analyses using facets (multi-coloured polygons; D, E, and F) and best-fit planes (green polygons; G, H, and I).

which is based on the rendering and visualization algorithm developed by Tarini et al. (2003), calculates the illumination of each point of the cloud as if the light was coming from a theoretical hemisphere around it. It generates a shade model that helps visualizing the surface characteristics and details of the point cloud. Additionally, the EDL tool enhances the perception of depth and surface features in point clouds applying non-photorealistic shading techniques (Boucheny and Ribes, 2011).

Considering that the notches in Re Tiberio Cave displayed sub-horizontal roofs and/or floors, our hypothesis was that the dip direction of those surfaces would mainly match the slope direction of the ancient water flow. In order to be able to systematically measure their spatial attitude in the point cloud we used the CloudCompare qFacets plugin (Dewez et al., 2016). This tool allows to segment point clouds into individual planar facets and measure their dip and dip direction (Fig. 3D-F). Only roof portions of the identified notches were considered for this analysis, as they displayed a more continuous and less disturbed profile with respect to the floor portions, often covered with sediments. The tool has two different algorithms capable of performing the segmentation, namely Kd-Tree and Fast Marching. Both algorithms divide the point cloud into smaller point groups, compute planar shapes within these aggregates, and gradually combine them into larger polygons (i.e., facets) based on a pre-selected fitting threshold. The main difference between these methods is that Kd-Tree conducts recursive subdivisions, which generates facets with different sizes, whereas Fast Marching takes a systematic approach and creates facets with similar sizes. Overall, Kd-Tree algorithm provided better results for the studied sectors of the cave. For consistency and reproducibility, we used the same Kd-tree cells fusion and facets frame parameters for all the notches: (1) maximum angle between neighbour polygons of 5°, (2) maximum distance between the merged polygons of 0.1 m, (3) 0.2 m as distance criterion (*Max. Distance @99*), (4) at least 10 points per facet, and (5) a maximum allowed facet contour of 0.2 m.

Additionally, we measured the dip and dip direction of the theoretical best-fit planes adjusted to the points of maximum curvature located at the inner end of each notch, i.e., the vertices of the pseudo-parabolic cross-sections of the notches (Fig. 3G-I). We generated these best-fit planes applying the 'trace tool' of the CloudCompare qCompass plugin (Thiele et al., 2017), which allows the semi-automatic digitalization of a trace following a least-cost path between sets of points manually selected in a point cloud, then computing a best-fit plane for the trace. Among other options, the least-cost path algorithm can be based on the mean curvature of the tracing area which allows to digitize ridges and valleys and, in this case, the innermost section of the notches. We could only apply this procedure to 63 % of the identified notches due to the relatively frequent lack of points in their deepest sections as a consequence of shadow areas associated with the restricted positioning of the TLS during the cave survey.

We exported the obtained spatial information into tables containing information on their relative (i.e., cave sector) and absolute (i.e., x-y-z coordinates) location, dip, and dip-direction. A geostatistical analysis was conducted with the DAISY3 software to calculate the mean attitude of the facets and the best-fit planes (Salvini et al., 1999; Salvini, 2004). This analysis was restricted to dip values smaller than 10° to target only the sub-horizontal surfaces potentially related to the ancient cave stream that carved the notches.

For each notch, we ran a polymodal statistical analyses (Gaussian fit) to extract the main systems of facets, calculating their dip and dip direction attributes. The results were plotted as lower-hemisphere stereograms. Then, we merged the main systems for each sector and extracted a mean attitude using the 'mean attitude' tool of DAISY3 software.

The mean attitude analyses have been performed using the same procedure for the dataset of the best-fit planes of each notch, grouped according to the cave sector they belong to. Sector S 1.3, given the scarcity of data, gave no results since best-fit planes could not be calculated. Sector S 3.3, on the other hand, shows only few best-fit planes ($n = 2$) without the possibility to run a mean attitude analysis with statistical significance.

Finally, we assessed the slope direction of the different clusters of notches identified in the 3D point cloud. Throughout the simultaneous evolution (downcutting) of the Senio valley and the Re Tiberio Cave system, notches belonging to the same generation would have been formed at altitudes similar to each other and different from those of other generations. Their overall slope is an indicator of the direction of the ancient water flow that formed them. We applied the automatic DBSCAN clustering algorithm (Ester et al., 1996) to group and define the different generations of notches along the cave based on the mean altitude of both their facets and best-fit planes. Contrary to other widely used clustering methods, DBSCAN can be applied without providing the number of clusters in advance. We considered a maximum vertical grouping distance of 0.4 m between all the facets, 0.15 m between the facets of the cluster number 4 which displayed a higher density of notches, and 0.8 m between best-fit planes. We calculated these distances with their respective elevation-based nearest neighbour graphs. Subsequently, we plotted the mean altitude of the notches against their horizontal distance to the outermost one, located at the entrance of the cave, and fitted a linear model for each cluster to use their best-fit lines to graphically solve the overall slope direction between notches belonging to the same DBSCAN cluster.

4. Results

4.1. Traditional cave survey

The five main sub-horizontal galleries identified in the topographic survey of the cave were analysed to calculate their average gradient (Fig. 4). All the analysed cave levels, which are formed by galleries with morphologies suggesting a flowing-water origin, are continuous and the most preserved in the entire cave system.

All these levels show an average gradient towards north-west, corresponding to the direction where the main cave entrance is found, with values ranging from 0.5 % to 6 % (Fig. 5). The lowest gradient (0.5 %) is observed in the main level, which is almost completely sub-horizontal. The tourist level, located few metres below the main one, shows a similar value (0.8 %). Both these levels, with calculated average gradients <1 %, cannot be used to infer any direction of the former flowing waters without a high level of uncertainty. The upper level, located around 225 m a.s.l., is slightly sloping towards W-NW with an average gradient of 3 %. Finally, the two lowest sub-horizontal galleries, one carved by the current active stream, are sloping towards W-NW with average gradients of 3 % and 6 %, respectively.

4.2. Geomorphological and sedimentological observations

As many gypsum caves in the area, the sub-horizontal passages are characterised by the presence of layered fluvial sediments, often with fining upward sequences distinctive of turbulent flow conditions of the underground river. These sediments, where they are still well preserved, fill horizontal recesses in the gypsum walls (notches) (Fig. 6A-E). Generally, each notch is filled by several fining upward sequences, each characterised from bottom to top by pebbles (up to 1 dm in diameter), coarse to fine sands, and finally silts-clays. In some of the sequences, but not always, the clays are topped by an up to 5 cm thick calcite flowstone layer.

Notches are generally freed of their sedimentary fills, showing their characteristic concave cross-section (Fig. 6B). Their depth spans from a couple of centimetres up to 1 m, topped by a close-to-horizontal roof (the planar facets in the laser scan data elaboration), and bounded downwards by a slightly sloping (10–30°) lower floor (Fig. 6C). In the main gallery (historical part), the highest passages have up to five generations of notches, topped by a close-to-horizontal wavy gypsum

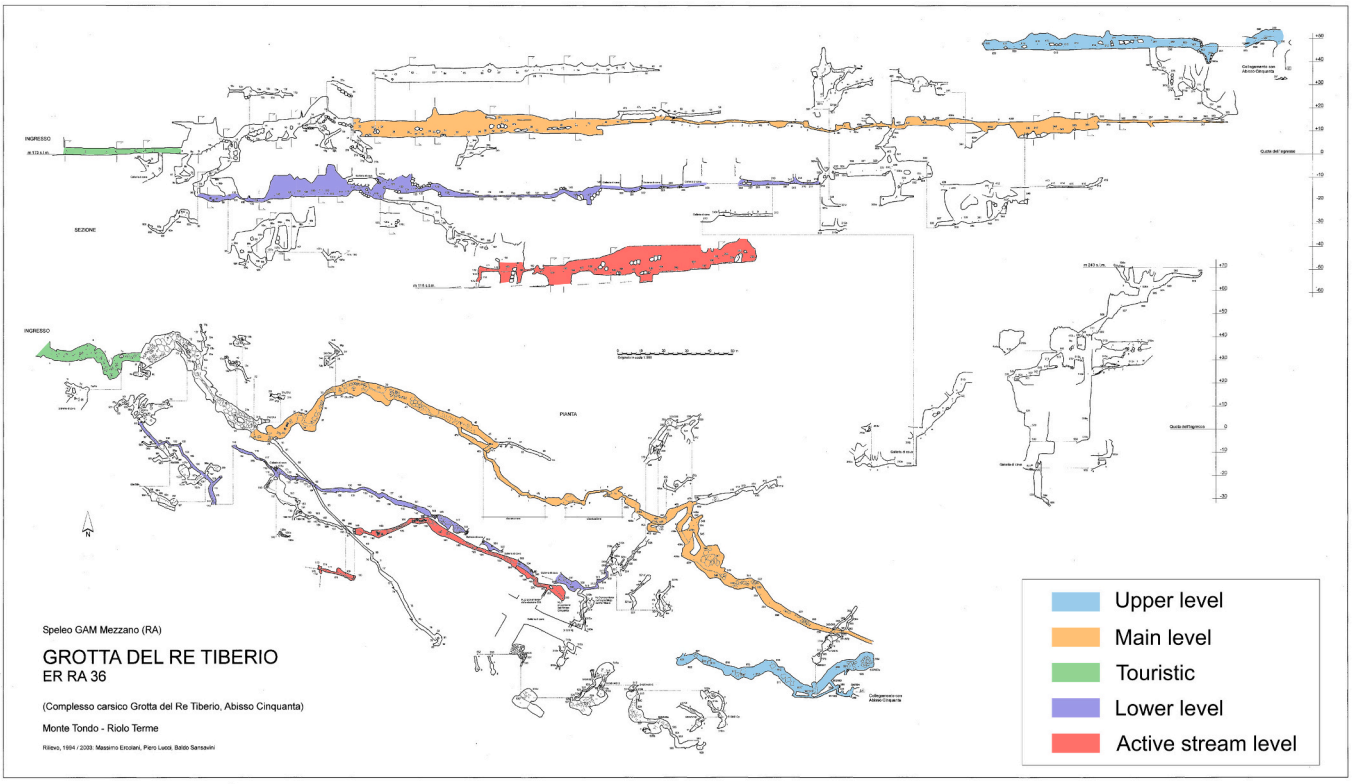

Fig. 4. Traditional topographic survey of the Re Tiberio Cave system. Five main sub-horizontal levels (Columbu et al., 2015) are highlighted with different colours in plan and longitudinal section view. These levels are characterised by the most continuous and well-developed karst conduits with morphologies suggesting a clear flowing-water origin, not obliterated by collapses or vadose entrenchment.

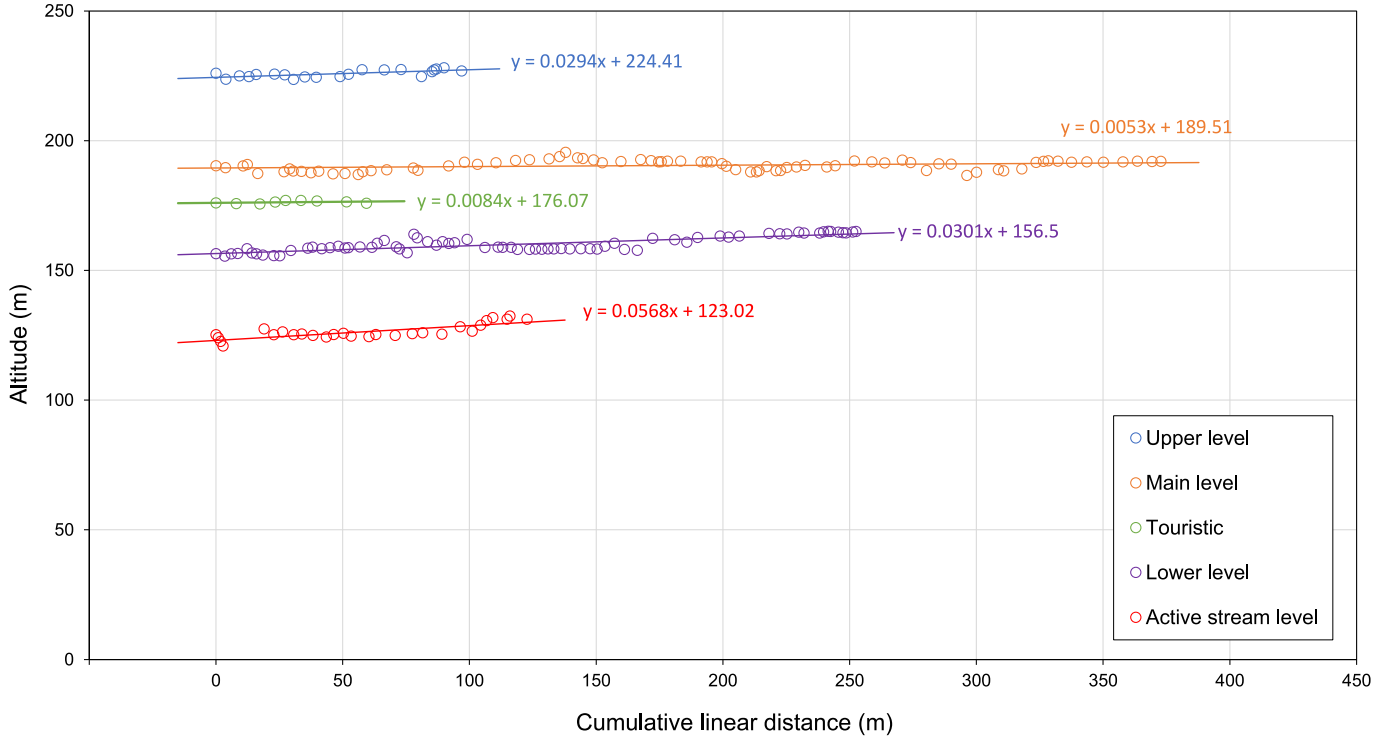

Fig. 5. Diagram plotting the cumulative linear distance vs. altitude of the cave survey points, extracted from the traditional topographic survey. Five main cave levels are identified and highlighted with different colours. The linear trendlines and their associated equations are displayed.

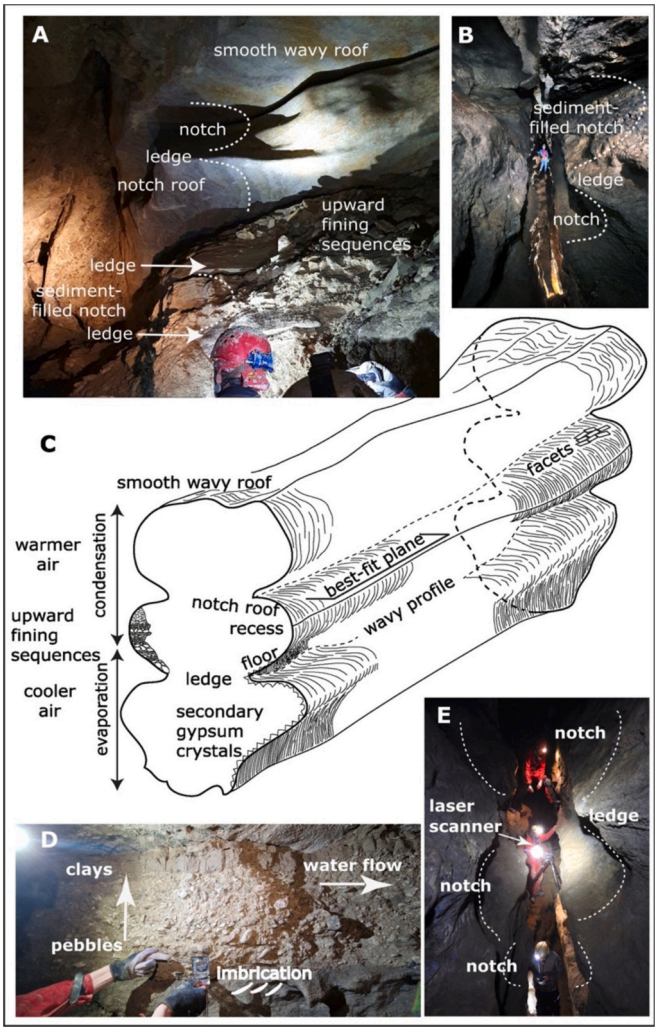

Fig. 6. Cave morphologies and sediments: A. Portion deep in Re Tiberio Cave, main level, with the smooth wavy roof, several notches and ledges, some of which filled with upward fining sequences (Photo Piero Gualandi); B. The historical branch in Re Tiberio, with notches and ledges well visible (Photo Piero Lucci); C. Schematic representation of the cave passage with notches and ledges and indication of other geomorphological and sedimentological features, in which the facets and best-fit planes used on the laser scan point clouds are shown; D. Picture of a upward-fining sedimentary sequence in the middle level of Re Tiberio Cave (just below the historical level), in which imbrication is clearly visible (finger points towards the cave entrance) (Photo Piero Gualandi); E. A mobile scanning session (BLK360 in hand of person in the centre of the photo) in a fracture-guided narrow passage with several notches (Photo Jorge Sevil-Aguareles).

roof. Here, secondary gypsum crystals are seen only in the lower parts of the passages, and especially on parts sticking out of the walls (e.g., ledges), whereas the upper parts and roof are smoothed.

Notches are separated from the under- or above lying notch by a ledge with sharp features (originally with angles of 20–30°, formed between the flat roof of the underlying notch and the sloping floor of the upper one). In a longitudinal profile notches appear to be almost horizontal but looking closely at the most continuous and long ones, they are slightly and variably inclined, being characterised by a wavy profile. This is especially visible in the ledges (which are more subject to later corrosion and erosion, and deposition of secondary gypsum crystals), but also following the imaginary line that connects the deepest recesses of the notches (the best-fit planes in the elaboration of the laser scan data).

Fluvial deposits, where preserved, especially in their pebbly portions, show imbrication. These indicators of flow show, for 90 % of the observations, a flow direction towards the present entrance of the cave (Fig. 6D).

4.3. Laser scan data

The combined use of three different laser scanners allowed for the reconstruction of a 3D model of the main gallery of Re Tiberio Cave even in its narrower and more complex portions (Fig. 7).

As a first step, the cave wall notches were extracted manually and using the ShadeVis and EDL tools in CloudCompare we were able to identify 84 notches within the walls of the studied passages of the cave. They are located at different elevations along the cave and displayed decametric to metric length and metric to decimetric width and depth. These have been statistically analysed as described in the methods section and a total 22,895 facets and 53 best-fit planes were measured in the 84 identified notches. Geostatistical analyses were performed to identify the facet's mean attitude and best fit planes of the cave wall notches in each of the 9 sectors in which the cave was subdivided (Fig. 8).

The mean attitude for each cave sector resulting from the polymodal geostatistical analysis of the facets and notches' best-fit planes would be consistent for the determination of the direction of the ancient water flow that generated them in each cave sector. It is important to note that not all the sectors of the point cloud provided data: (1) We identified 4 notches in sector 1.3 but only 12 facets displayed dip values lower than 10° and, taking into account that the minimum number of facets identified per sector was 164, we considered that those of sector 1.3 would not provide statistically significant data. (2) Additionally, the sinuosity and narrowness of sector 1.3 and the resulting restrictions on the positioning of the TLS caused the point cloud to exhibit numerous shadow zones which prevented us from calculating any best-fit plane of the notches. (3) This same problem restricted the analysis of the best-fit planes in sector 3.3, where we only managed to digitize the maximum curvature trace of two out of six notches identified there.

Fig. 8A displays the mean attitude of the sub-horizontal facets modelled in the notches within each sector of the 3D point cloud. Dips and dip directions range from 0.9° to 3.6° and from 27° to 319°, respectively. Based on the modelled sub-horizontal facets and taking into account the orientation of the cave sectors, the mean attitude of the notches of 5 out of 8 statistically significant sectors (63 %: S1.1, S1.2, S2.1, S3.1, and S3.3) display dip directions towards the current entrance of the cave.

On the other hand, Fig. 8B shows the mean attitude of the best-fit planes modelled across the maximum curvature section of the notches' profile. In this case, the mean dip direction of the best-fit planes did not provide conclusive results. The mean notches' best-fit planes of sector 1.2 are directed towards the entrance, whereas those of sector 2.3 pointed in the other direction (into the mountain). Additionally, the mean notches' best-fit planes of all the other statistically significant sectors displayed dip directions perpendicular or oblique to the overall orientation of the cave passage (i.e. nor directing towards the entrance nor inside the mountain).

The spatial analysis of the slope direction between notches belonging to the same DBSCAN cluster based on the mean altitude of sub-horizontal facets revealed that 5 out of 7 clusters (71 %) display a slope direction towards the current entrance of the cave (Fig. 9A). We increased the resolution of the clustering analysis for cluster 4 because of the high density of notches between 189 and 193 m a.s.l., an elevation range consistent with that of the most developed sectors of the gallery scanned in the Re Tiberio Cave (main level) (Fig. 2). Fig. 9B shows the result of this higher-resolution analysis where 4 out of 6 clusters (66 %) exhibit slope directions towards the entrance of the cave.

On the contrary, this same analysis but based on the altitude of the best-fit planes yielded less consistent data, with the 6 identified clusters displaying an equal distribution of outward and inward slope directions

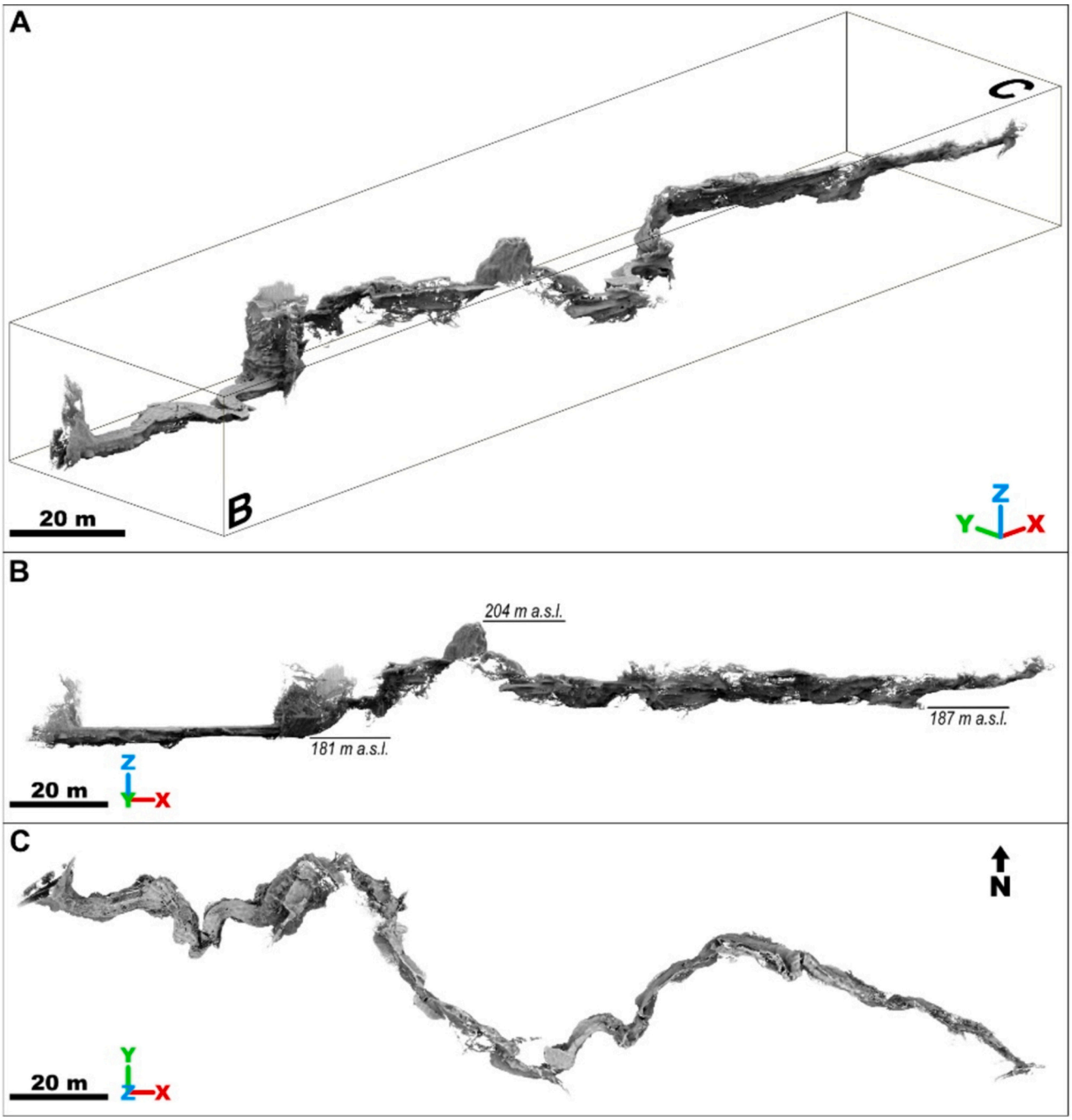

Fig. 7. Compound 3D point cloud of the scanned passage of the Re Tiberio Cave resulted from the TLS survey: (A) isometric, (B) profile, and (C) plan views. Note the existence of scattered points on some of the edges of the model, which are related to the existence of shadow zones caused by the positioning restrictions of the scanner along the cave.

(Fig. 9C).

5. Discussion

By combining fixed and mobile laser scanners we were able to compare these technologies in a complex cave environment. The resolution of the obtained data is different between the two technologies (the fixed TLS data are much more defined) but combining both (fixed and mobile) it is possible to get high quality surveys (floor plans, long profiles and cross-sections) of all (narrow and large) passages of the cave.

From a practical point of view, both fixed and mobile TLS instruments need lights to obtain coloured data of the cave environment, but a dedicated set up of spotlights is necessary for fixed TLS, while lighting directed the area where the mobile instrument is used is sufficient in the case of the BLK360 (when it is handheld) and the BLK2GO. As described in the previous paragraph, the two technologies (fixed and mobile) are certainly different and have limits due to their shapes and sizes. Fixed TLS can guarantee to obtain data in large and high areas (having a long range), but their use can be limited by the morphologies (and size) of the cave passages. On the other hand, mobile (hand-held) scanners can also be used in small and narrow environments, but their range is limited to a few tens of metres. This means that in very large cave environments the use of these mobile TLSs must be carefully evaluated.

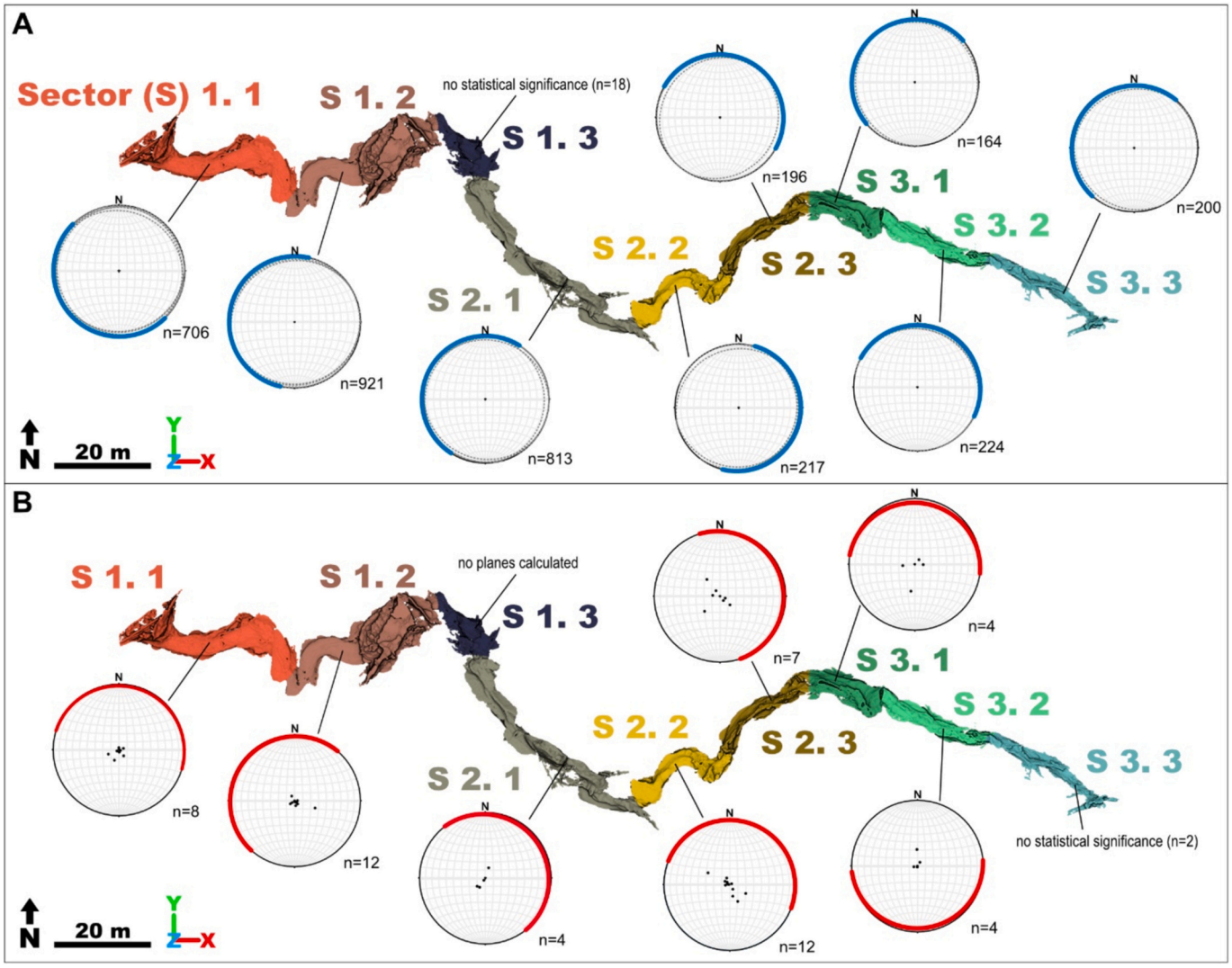

Fig. 8. Results of the geostatistical analysis of the mean dip and dip direction of (A) the sub-horizontal (< 10°) facets (in blue) and (B) the best-fit planes (in red) of the notches modelled in the different sectors of the scanned gallery of the Re Tiberio Cave. Stereograms of (A) show the main systems of facets identified by polymodal Gaussian-fit analysis with dashed lines.

Regarding the potential of TLS for conducting detailed cave morphometric analyses, the overall quality and completeness of the 3D point cloud is a major limiting factor capable of constraining any further analysis. The main difference between the point clouds obtained by means of these two types of scanners is that surfaces of the fixed TLS display less noise. Therefore, despite the advantages of mobile laser scanners such as the used Leica BLK 360 and BLK2GO, both allowing to capture data on the go even along narrow and sinuous galleries, the resulting less-precise 3D point clouds (e.g., Del Duca and Machado, 2023) may have negatively affected the planar facets modelled by the qFacets plugin (Dewez et al., 2016) for segmenting the point cloud. This is an important factor to consider when designing new TLS scanning campaigns. Additionally, the incompleteness of the point cloud did limit our results. The narrowness and sinuosity of most of the scanned galleries of the Re Tiberio Cave system, together with the size and the associated positioning restrictions of the Leica ScanStation P50 TLS, resulted in the presence of shadow zones in the deepest sectors of the notches recorded in the point cloud. These empty areas affected the digitalisation of the maximum curvature traces along the innermost section of the notches and, consequently, we were not able to calculate the best-fit planes of 37 % of the notches. A more thorough scanning process (with handheld scanners) could reduce shadow problems in some areas, but it would also increase the time required for data acquisition and lead to greater data redundancy. Nevertheless, most probably certain areas in the cave would still pose challenges for relatively large scanners due to positioning, distance-to-surface, and line-of-sight constraints, which are common problems encountered in the scanning of caves by means of laser scanners (e.g., Gallay et al., 2015; Fabbri et al., 2017; Pfeiffer et al., 2023).

Despite these restrictions, the general results from the study of the notches of the Re Tiberio Cave support its sloping towards the actual entrance, and thus its ancient function as a spring. The geostatistical analyses of the mean attitude of the modelled planar facets revealed that the mean dip direction of 63 % of the notches point towards the present entrance. In addition, the DBSCAN clustering of the facets showed that, with the exception of cluster n. 6, the best-fit lines for each cluster also slope towards the current cave entrance. However, not all the applied methods provided equally robust data. The mean attitude and clustering slope of the modelled best-fit planes did not provide conclusive data. As described above, they display mean dip directions both pointing downstream and upstream and, in some cases, even obliquely to their respective sectors. Overall, the qFacets analysis provided more abundant and consistent data than the method based on the best-fit planes of the notches. We attribute this to two main factors: (1) the quality and

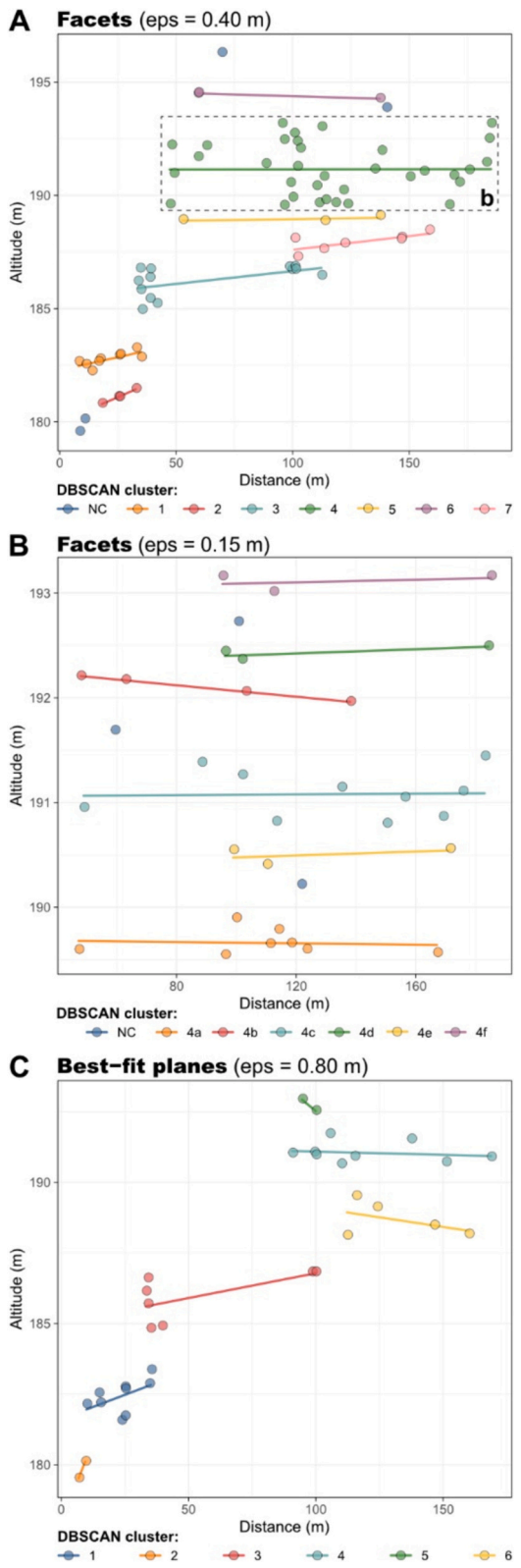

Fig. 9. Altitude-based clustering analyses conducted with the DBSCAN algorithm (Ester et al., 1996) for the mean altitude of (A and B) the subhorizontal facets and (C) the best-fit planes of the notches identified in the scanned gallery of the Re Tiberio Cave. (B) High-resolution clustering analysis of the general cluster 4 of subfigure 'A'. The x-axes refer to the horizontal distance to the outermost notch identified from the cave entrance. The DBSCAN eps (epsilon) value is the maximum vertical grouping distance between notches calculated with the respective nearest neighbour graphs. Note the best-fit lines used to determine the general slope direction between the notches of the DBSCAN clusters.

completeness of the point cloud have less influence on the calculation of planar facets compared to the best-fit planes, where insufficient data, namely shadow zones, may result in the best-fit plane trace not passing the area of highest curvature, not being representative of the entire notch, or not being computed at all. (2) The data processing methods themselves, as the qFacets plugin is automatic and the best-fit plane tracing, although semi-automatically assisted, still requires the manual selection of waypoints and thus allows for human biases. Furthermore, additional errors may arise from the data acquisition and registrations of the 3D point cloud, such as small deviations related to TLS levelling inside the cave or those associated with laser-surface geometric interaction and surface humidity properties (e.g., Giordan et al., 2021; Muralikrishnan, 2021), the modelling of facets and best-fit planes, and even the erosion or condensation-corrosion phenomena during late speleogenetic stages (e.g., Columbu et al., 2021). These disturbances may alter the modelled surfaces of the notches in some sectors of the cave and result in small changes in the dip and dip direction of the modelled surfaces, which can have significant consequences on the conclusions derived from the analyses of such sub-horizontal data.

The analysis of the average gradient using the original cave survey appears to confirm the overall results of the laser scan data. The five main levels are all inclined towards the entrance of the cave, with values ranging from 0.5 to 6 %. It must be taken into account that the traditional cave survey data uses the available and explorable space inside the cave, and the original shape of the passages is disturbed by sediment fills, rockfalls, and spaces too narrow to cross. However, the consistency of the survey data, all indicating an albeit very low inclination towards the entrance, gives us confidence in concluding that the cave passages indeed slope towards the Senio River valley. This fact is further strengthened by the observations on imbrication of the still present sedimentary fills, 9 out of 10 indicate a flow direction towards the entrance. The few exceptions, where imbrication indicates a flow into the mountain, can often be explained by reworking of older sediments in areas where two superimposed levels are connected with shafts.

6. Conclusions

Laser scan surveys in caves, and the elaboration of point clouds, are increasingly used in resolving speleogenetic and morphogenetic problems, where traditional mapping methods often fall short. Laser scan data have much higher resolution than traditional cave surveys, although complete coverage of all recesses on cave walls and roofs remains challenging due to both physical and technical constraints. The combined use of fixed and mobile laser scanners, with different sizes, resolutions, and manageability, allows to expand the coverage, and scan also narrow and tortuous passages. Laser scanning is also often less time-consuming than traditional cave mapping, and the higher accuracy and resolution are great advantages, especially in geomorphological studies.

The combination of statistical data, based on the detailed elaboration of the point cloud, especially notch roofs (facets) and the best-fit planes connecting the notches' deepest recesses, the simple analysis of the traditional cave map (profile), and geomorphological-sedimentological observations (i.e. imbrication of sediments) has allowed to infer the general inclination of the cave passages, all inclined towards the present entrance (and the Senio River valley). The Re Tiberio Cave system was thus a resurgence, with a recharge area located East, and a general flow direction from ESE to WNW.

CRediT authorship contribution statement

Jorge Sevil-Aguareles: Writing – review & editing, Writing – original draft, Visualization, Methodology, Investigation, Formal analysis,

Data curation, Conceptualization. **Luca Pisani:** Writing – review & editing, Writing – original draft, Visualization, Methodology, Investigation, Formal analysis, Data curation. **Veronica Chiarini:** Writing – review & editing, Writing – original draft, Visualization, Investigation. **Tommaso Santagata:** Writing – review & editing, Writing – original draft, Software, Resources, Methodology, Data curation. **Jo De Waele:** Writing – review & editing, Writing – original draft, Supervision, Resources, Project administration, Investigation, Funding acquisition, Conceptualization.

Declaration of competing interest

The authors declare that they have no known competing financial interests or personal relationships that could have appeared to influence the work reported in this paper.

Acknowledgements

The authors would like to thank the many cavers that helped us during our surveys in the Re Tiberio cave, and especially those that gave permission to use their pictures (Piero Lucci, Piero Gualandi, Martin Arriolabengoa). Piero Lucci is also thanked for drawing Fig. 1. The "*Parco Regionale della Vena del Gesso Romagnola*" is thanked for the authorisation given to study the cave, and so is the Association "La Nottola APS-ASD" who manages the cave visits and helped during our surveys. Thanks to the Speleo GAM Mezzano, and especially Massimo Ercolani, Piero Lucci and Garibaldi (Baldo) Sansavini for having given us the original cave map. Virtual Geographic Agency is acknowledged for the acquisition of the cave using three different terrestrial laser scanners. Finally, the authors would also like to thank Francesco Ardito for his collaboration in the preparation of the TLS data. During data collection and analysis phases, JSA had a pre-doctoral contract (PRE2018-084240) cofinanced by the Spanish Government and the European Social Fund (ESF).

Data availability

Data will be made available on request.

References

Audra, P., Palmer, A.N., 2015. Research frontiers in speleogenesis. Dominant processes, hydrogeological conditions and resulting cave patterns. Acta Carsologica 44, 315–348. https://doi.org/10.3986/ac.v44i3.1960.

Boucheny, C., Ribes, A., 2011. Eye-dome lighting: a non-photorealistic shading technique. The Source Issue. 17. Kitware Blog. https://blog.kitware.com/eye-dome-lighting-a-non-photorealistic-shading-technique/.

Cailhol, D., Audra, P., Nehme, C., Nader, F.H., Garašić, M., Heresanu, V., Gucel, S., Charalambidou, I., Satterfield, L., Cheng, H., Edwards, R.L., 2019. The contribution of condensation-corrosion in the morphological evolution of caves in semi-arid regions: preliminary investigations in the Kyrenia range, Cyprus. Acta Carsologica 48 (1), 5–27. https://doi.org/10.3986/ac.v48i1.6782.

Calaforra, J.M., Gázquez, F., 2017. Gypsum speleogenesis: a hydrogeological classification of gypsum caves. Int. J. Speleol. 46 (2), 251. https://doi.org/10.5038/1827-806X.46.2.2125.

Calvet, M., Gunnell, Y., Braucher, R., Hez, G., Bourles, D., Guillou, V., Delmas, M., Aster Team, 2015. Cave levels as proxies for measuring post-orogenic uplift: evidence from cosmogenic dating of alluvium-filled caves in the French Pyrenees. Geomorphology 246, 617–633. https://doi.org/10.1016/j.geomorph.2015.07.013.

Canevese, E.P., Forti, P., Tedeschi, R., 2013. New acquisition, 3D modeling, and data used methods: The laser scanning survey of Retiberio Cave. In: Filippi, M., Bosak, P. (Eds.), Proceedings 16th International Congress of Speleology, Brno, vol. 2, pp. 340–345.

Chiarini, V., Columbu, A., Pisani, L., De Waele, J., 2022. L'importanza del sistema carsico del Re Tiberio nel definire il modello di evoluzione dei paesaggi nei gessi: il Progetto EvolGyps. In: Ercolani, M., Lucci, P., Piastra, S. (Eds.), Atti del Convegno "La Grotta del Re Tiberio. Valori ambientali e valori culturali", Faenza, Memorie dell'Istituto Italiano di Speleologi, Serie II, vol. 41, pp. 35–48.

Chiarini, V., Pisani, L., Columbu, A., De Waele, J., 2024. EvolGyps Landscape evolution in the Messinian gypsum areas of Emilia-Romagna. Memorie dell'Istituto Italiano di Speleologia (Bologna), Serie II, vol. 46A, pp. 1–182.

CloudCompare (version 2.13) [GPL software], 2024. Retrieved from. http://www.cloudcompare.org/.

Columbu, A., De Waele, J., Forti, P., Montagna, P., Picotti, V., Pons-Branchu, E., Hellstrom, J., Bajo, P., Drysdale, R.N., 2015. Gypsum caves as indicators of climate-driven river incision and aggradation in a rapidly uplifting region. Geology 43 (6), 539–542. https://doi.org/10.1130/G36595.1.

Columbu, A., Chiarini, V., De Waele, J., Drysdale, R.N., Woodhead, J., Hellstrom, J., Forti, P., 2017. Late quaternary speleogenesis and landscape evolution in the northern Apennine evaporite areas. Earth Surf. Process. Landf. 42 (10), 1447–1459. https://doi.org/10.1002/esp.4099.

Columbu, A., Audra, P., Gázquez, F., D'Angeli, I.M., Bigot, J.-Y., Koltai, G., Chiesa, R., Yu, T.L., Hu, H.-M., Shen, C.-C., Carbone, C., Heresanu, V., Nobécourt, J.-C., De Waele, J., 2021. Hypogenic speleogenesis, late stage epigenic overprinting and condensation-corrosion in a complex cave system in relation to landscape evolution (Toirano, Liguria, Italy). Geomorphology 376, 107561. https://doi.org/10.1016/j.geomorph.2020.107561.

De Waele, J., Gutiérrez, F., 2022. Karst Hydrogeology, Geomorphology and Caves. John Wiley and Sons, Chichester. https://doi.org/10.1002/9781119605379, 888 p.

De Waele, J., Ferrarese, F., Granger, D., Sauro, F., 2012. Landscape evolution in the Tacchi area (central-east Sardinia, Italy) based on karst and fluvial morphology and age of cave sediments. Geogr. Fis. Din. Quat. 35 (2), 119–127. https://doi.org/10.4461/GFDQ.2012.35.11.

De Waele, J., Fabbri, S., Santagata, T., Chiarini, V., Columbu, A., Pisani, L., 2018. Geomorphological and speleogenetical observations using terrestrial laser scanning and 3D photogrammetry in a gypsum cave (Emilia Romagna, N. Italy). Geomorphology 319, 47–61. https://doi.org/10.1016/j.geomorph.2018.07.012.

Del Duca, G., Machado, C., 2023. Assessing the Quality of the Leica BLK2GO Mobile Laser Scanner versus the Focus 3D S120 Static Terrestrial Laser Scanner for a Preliminary Study of Garden Digital Surveying. Heritage 6 (2), 1007–1027. https://doi.org/10.3390/heritage6020057.

Dewez, T.J.B., Girardeau-Montaut, D., Allanic, C., Rohmer, J., 2016. Facets: a Cloudcompare plugin to extract geological planes from unstructured 3D point clouds. Int. Arch. Photogramm. Remote Sens. Spatial Inf. Sci. XLI-B5, 799–804. https://doi.org/10.5194/isprs-archives-XLI-B5-799-2016.

Ester, M., Kriegel, H.-P., Sander, J., Xu, X., 1996. A density-based algorithm for discovering clusters in large spatial databases with noise. In: KDD-96 Proceedings, pp. 226–231. https://www.aaai.org/Papers/KDD/1996/KDD96-037.

Fabbri, S., Sauro, F., Santagata, T., Rossi, G., De Waele, J., 2017. High-resolution 3-D mapping using terrestrial laser scanning as a tool for geomorphological and speleogenetical studies in caves: an example from the Lessini mountains (North Italy). Geomorphology 280, 16–29. https://doi.org/10.1016/j.geomorph.2016.12.001.

Fabbri, S., Chiarini, V., Ercolani, M., Sansavini, G., Santagata, T., De Waele, J., 2021. Terrestrial laser scanning, geomorphology and archaeology of a Roman gypsum quarry (Vena del Gesso Romagnola area, Northern Apennines, Italy). J. Archaeol. Sci. Rep. 36, 102810. https://doi.org/10.1016/j.jasrep.2021.102810.

Farrant, A.R., Smart, P.L., 2011. Role of sediment in speleogenesis; sedimentation and paragenesis. Geomorphology 134 (1–2), 79–93. https://doi.org/10.1016/j.geomorph.2011.06.006.

Ford, D.C., Williams, P.W., 2007. Karst Hydrogeology and Geomorphology. John Wiley and Sons, Chichester. https://doi.org/10.1002/9781118684986, 567 p.

Gallay, M., Kaňuk, J., Hochmuth, Z., Meneely, J.D., Hofierka, J., Sedlák, V., 2015. Large-scale and high-resolution 3-D cave mapping by terrestrial laser scanning: a case study of the Domica Cave, Slovakia. International Journal of Speleology 44 (3), 277–291. https://doi.org/10.5038/1827-806X.44.3.6.

Giordan, D., Godone, D., Baldo, M., Piras, M., Grasso, N., Zerbetto, R., 2021. Survey solutions for 3D acquisition and representation of artificial and natural caves. Appl. Sci. 11 (14), 6482. https://doi.org/10.3390/app11146482.

Harmand, D., Adamson, K., Rixhon, G., Jaillet, S., Losson, B., Devos, A., Hez, G., Calvet, M., Audra, P., 2017. Relationships between fluvial evolution and karstification related to climatic, tectonic and eustatic forcing in temperate regions. Quat. Sci. Rev. 166, 38–56. https://doi.org/10.1016/j.quascirev.2017.02.016.

Haüselmann, P., Granger, D.E., Jeannin, P.Y., Lauritzen, S.E., 2007. Abrupt glacial valley incision at 0.8 Ma dated from cave deposits in Switzerland. Geology 35 (2), 143–146. https://doi.org/10.1130/G23094A.

Heeb, B., 2014. The Next Generation of the DistoX Cave Surveying Instrument. CREG Journal 88, 5–8.

Klimchouk, A.B., 1996. The dissolution and conversion of gypsum and anhydrite. International Journal of Speleology 25 (3), 21–36. https://doi.org/10.5038/1827-806X.25.3.2.

Lugli, S., Manzi, V., Roveri, M., 2008. New facies interpretation of the Messinian evaporites in the Mediterranean. In: CIESM Workshop Monographs, 33, pp. 67–72.

Muralikrishnan, B., 2021. Performance evaluation of terrestrial laser scanners - a review. Meas. Sci. Technol. 32 (7), 072001. https://doi.org/10.1088/1361-6501/abdae3.

Pasini, G., 2009. A terminological matter: paragenesis, antigravitative erosion or antigravitational erosion? International Journal of Speleology 38 (2), 129–138. https://doi.org/10.5038/1827-806X.38.2.4.

Pfeiffer, J., Rutzinger, M., Spötl, C., 2023. Terrestrial laser scanning for 3D mapping of an alpine ice cave. Photogramm. Rec. 38 (181), 6–21. https://doi.org/10.1111/phor.12437.

Pisani, L., Lucci, P., 2022. Le grotte e i sistemi carsici di Monte Tondo. Una ricostruzione 3D tramite il software cSurvey. In: Ercolani, M., Lucci, P., Piastra, S., del Convegno, Atti (Eds.), La Grotta del Re Tiberio. Valori ambientali e valori culturali. Memorie dell'Istituto Italiano di Speleologi, Faenza, pp. 49–54. Serie II 2022.

Pisani, L., Antonellini, M., De Waele, J., 2019. Structural control on epigenic gypsum caves: evidences from Messinian evaporites (Northern Apennines, Italy). Geomorphology 332, 170–186. https://doi.org/10.1016/j.geomorph.2019.02.016.

Rixhon, G., 2023. Deeper underground: Cosmogenic burial dating of cave-deposited alluvium to reconstruct long-term fluvial landscape evolution. Earth Sci. Rev. 239, 104357. https://doi.org/10.1016/j.earscirev.2023.104357.

Roveri, M., Manzi, V., Ricci Lucchi, F., Rogledi, S., 2003. Sedimentary and tectonic evolution of the Vena del Gesso basin (Northern Apennines, Italy): Implications for the onset of the Messinian crisis. GSA Bull. 114 (4), 387–405. https://doi.org/10.1130/0016-7606(2003)115%3C0387:SATEOT%3E2.0.CO;2.

Salvini, F., 2004. Daisy 3: The Structural Data Integrated System Analyzer Software. University of Roma Tre, Rome available at: http://host.uniroma3.it/progetti/fralab/Downloads/Programs/.

Salvini, F., Billi, A., Wise, D.U., 1999. Strike-slip fault-propagation cleavage in carbonate rocks: the Mattinata fault zone, Southern Apennines, Italy. J. Struct. Geol. 21, 1731–1749. https://doi.org/10.1016/S0191-8141(99)00120-0.

Sanna, L., Chiarini, V., De Waele, J., 2023. Underground Geodiversity of Italian Show Caves: an Overview. Geoheritage 15 (4), 126. https://doi.org/10.1007/s12371-023-00876-z.

Santagata, T., Lugli, S., Camorani, M.E., Ercolani, M., 2015. Laser scanner survey and tru view applications of the" Grotta della lucerna"(Ravenna, Italy), a roman mine for lapis specularis. Opera Ipogea 1, 411–416.

Santagata, T., Brunelli, V., Bergianti, S., 2022a. 3D cave mapping with hand-held and terrestrial laser scanning. In: Proceedings 18th International Congress of Speleology, Savoie Mont Blanc, Karstologia Mémoires, 26, pp. 55–58.

Santagata, T., Sharatmiadari, Y., Colavita, L., 2022b. Photogrammetry and Terrestrial Laser Scanning of diapirs and salt caves in Iran. In: Proceedings 18th International Congress of Speleology, Savoie Mont Blanc, Karstologia Mémoires, 26, pp. 59–62.

Tarini, M., Cignoni, P., Scopigno, R., 2003. Visibility based methods and assessment for detail-recovery. In: Proceedings of the IEEE Visualization Conference “VIS’03”. IEEE, 457-464. https://doi.org/10.1109/VISUAL.2003.1250407.

Thiele, S.T., Grose, L., Samsu, A., Micklethwaite, S., Vollgger, S.A., Cruden, A.R., 2017. Rapid, semi-automatic fracture and contact mapping for point clouds, images and geophysical data. Solid Earth 8 (6), 1241–1253. https://doi.org/10.5194/se-8-1241-2017.

Urban, J., Andreychouk, V., Kasza, A., 2009. Epigene and hypogene caves in the Neogene gypsum of the Ponidzie area (Niecka Nidziańska region), Poland. In: Klimchouk, A., Ford, D. (Eds.), Hypogene Speleogenesis and Karst Hydrology of Artesian Basins. Ukrainian Inst. Speleology and Karstology, Simferopol, pp. 223–231.

Vigna, B., D’Angeli, I.M., Fiorucci, A., De Waele, J., 2017. Hydrogeological flow in gypsum karst areas: some examples from northern Italy and main circulation models. International Journal of Speleology 46 (2), 205–217. https://doi.org/10.5038/1827-806X.46.2.2095.

White, W.B., 2002. Karst hydrology: recent developments and open questions. Eng. Geol. 65 (2–3), 85–105. https://doi.org/10.1016/S0013-7952(01)00116-8.